THE JOURNAL OF PROSTHETIC DENTISTRY

RESEARCH AND EDUCATION

Anomaly detection of screw loosening of different implant-abutment connection designs using resonance frequency analysis: An in vitro study

Sara Reda Sammour, MDS,[a] Hideki Naito, PhD,[b] Ryuji Shigemitsu, DDS, PhD,[c] Ziqi Xie, MDS,[d] Tomoyuki Kimoto, PhD,[e] Keiichi Sasaki, DDS, PhD,[f] Nobuhiro Yoda, DDS, PhD,[g] and Toru Ogawa, DDS, PhD[h]

ABSTRACT

Statement of problem. Screw loosening is a common mechanical complication in implant-supported restorations, yet early detection remains challenging because of the lack of noninvasive, quantitative assessment tools.

Purpose. This in vitro study aimed to evaluate the ability of resonance frequency analysis (RFA) combined with machine learning techniques to detect screw loosening in 3 implant–abutment connection designs: conical, internal tri-channel, and external hexagonal.

Material and methods. Three connection types were tested using 6 implants inserted into mandibular jaw models. RFA was conducted using a triaxial accelerometer under 7 loosening conditions with the frequency responses in the x, y, and z directions being recorded. Supervised learning (random forest) was used for binary (intact versus abnormal) and multiclass (7 classes) classification. Unsupervised learning was used to detect anomalies.

Results. The RFA revealed unique vibrational profiles for each connection design. The random forest classifier achieved 100% accuracy in binary classification and 83% to 92% in multiclass classification. Feature importance analysis highlighted the relevance of the triaxial vibration data. The convolutional autoencoder consistently identified screw loosening as early as 5 degrees.

Conclusions. RFA combined with machine learning reliably detected screw loosening across various types of implant-abutment connections. This method offers a noninvasive, quantitative tool for the early detection of mechanical complications in implant dentistry. (J Prosthet Dent 2026;135:954.e1-e14)

Screw loosening is a prevalent mechanical complication of implant-supported prostheses that occurs in 4.3% to 10% of patients, typically after functional loading.[1] Screw loosening can lead to problems that include implant-abutment instability, pain, increased risk of bacterial infiltration, peri-implantitis, and potentially marginal bone loss.[1,2] Factors contributing to screw loosening include inadequate initial torque, unfavorable occlusal forces, cantilever extensions, material fatigue, microleakage, parafunctional habits, crestal bone resorption, and implant-related characteristics.[3,4] To mitigate screw loosening, clinicians should focus on appropriate treatment planning, implant positioning, prosthesis design, and achieving even occlusal force distribution while also conducting regular follow-ups to detect and address early signs of loosening.[5]

In clinical practice, screw loosening is often detected only after patients report discomfort or when clinicians

Supported in part by the Terumo Life Science Foundation (Grant Number: 24-II1001).
The authors declare no conflicts of interest related to this study.

[a]PhD student, Division of Advanced Prosthetic Dentistry, Tohoku University Graduate School of Dentistry, Sendai, Japan; and Assistant Lecturer, Prosthodontic Department, Faculty of Dentistry, Tanta University, Tanta, Egypt.
[b]Associate Professor, Department of Civil and Environmental Engineering, Tohoku University Graduate School of Engineering, Sendai, Japan.
[c]Assistant Professor, Liaison Center for Innovative Dentistry, Division for Advanced Education Development, Tohoku University Graduate School of Dentistry, Sendai, Japan.
[d]PhD student, Division of Advanced Prosthetic Dentistry, Tohoku University Graduate School of Dentistry, Sendai, Japan.
[e]Associate Professor, Department of Electrical and Electronic Engineering, National Institute of Technology, Oita College, Oita, Japan.
[f]Professor, Graduate School of Dentistry, Tohoku University, Sendai, Japan.
[g]Professor, Division of Advanced Prosthetic Dentistry, Tohoku University Graduate School of Dentistry, Sendai, Japan.
[h]Professor, Division of Comprehensive Dentistry, Tohoku University Graduate School of Dentistry, Sendai, Japan.

Clinical Implications

RFA combined with machine learning enabled early, the noninvasive detection of screw loosening across different implant–abutment connections. This approach allowed timely intervention before clinical mobility, reducing the risk of prosthetic complications and bone loss, and provided quantitative, reproducible assessments to support objective clinical decision-making.

observe prosthesis movement.[6] For single crowns, this typically occurs after the superstructure becomes loose, while, in splinted restorations, early loosening may go unnoticed because of support from adjacent units. Conventional mobility evaluations are subjective and may fail to detect partial loosening.[7] The interval between onset and detectable mobility has been poorly defined, highlighting the need for noninvasive, quantitative methods such as resonance frequency analysis (RFA) for the earlier and more objective detection of mechanical instability.[8,9]

RFA is a noninvasive, objective method that is widely used in implant dentistry to assess implant stability. It measures the vibration frequency of an implant, expressed as Implant Stability Quotient (ISQ) units.[10,11] Because screw loosening also alters the connection state between implant components, RFA can detect early mechanical instability.[12] Its reliability is supported by correlations with traditional mechanical tests such as peak torque and pull-out force, and its use has been extended to polyaxial pedicle screws in orthopedics.[13,14]

Despite its advantages, RFA readings can be influenced by bone quality, implant design and material, soft tissue condition, and patient-specific factors, as well as measurement and environmental variability.[15] Advanced data analysis methods, particularly machine learning algorithms, can help improve the accuracy and reliability of RFA assessments.

Machine learning algorithms have emerged as powerful tools for analyzing complex data in dentistry.[16] They can be broadly categorized into supervised approaches, such as neural networks and random forests, trained on labeled data to predict outcomes,[17] and unsupervised approaches, which detect patterns without labeled data.[18] Recent studies have applied these methods to fixed dental prostheses (FDPs). For example, Qi et al[19] combined RFA with finite element modeling to investigate cement degradation but faced difficulty identifying RFA features that reflected loosening. Sammour et al[20] addressed this by applying both supervised and unsupervised learning to FDP models, showing that RFA features can reliably detect early retention loss. However, these studies focused on prosthesis retention (cement loss) rather than implant–abutment screw loosening.

The authors are unaware of a previous study that applied RFA combined with machine learning to detect screw loosening in different implant–abutment connection (IAC) designs. By integrating machine learning, the present work enhanced the analysis and comparison of RFA data across connection types, addressing a clinically relevant mechanical complication. The null hypothesis was that RFA, even when combined with machine learning, would not reliably detect early screw loosening across different IAC designs.

MATERIAL AND METHODS

Three distinct implant abutment connection (IAC) designs were tested: a conical connection (NobelParallel CC; Nobel Biocare), an internal tri-channel connection (Replace Select Tapered; Nobel Biocare), and an external hexagonal connection (Brånemark System Mk III; Nobel Biocare). All implants had a standardized length of 10 mm; the conical and internal tri-channel implants had a diameter of 4.3 mm, while the external hexagonal implant measured 4.0 mm in diameter. Three jaw models (EX-7 and 1017A; Nissin) were prepared, with each model receiving 2 implants at the first molar site (Fig. 1). Implant positioning was standardized by using a custom-made surgical guide to ensure accuracy (Fig. 2).

RFA measurements were conducted using a triaxial piezoelectric pickup sensor (Model 3133A1; Dytran Instruments, Inc), power unit (Model 4114B1; Dytran Instruments, Inc), PowerLab data acquisition system (Model ML880; Dytran Instruments, Inc), and a software package (LabChart 7; Dytran Instruments, Inc).[10] The 3-dimensional accelerometer sensor was securely mounted on the lingual surface of the abutment cap or jig (Fig. 3). Vibrations were applied buccolingually at 4 Hz with an implant stability tester (Periotest Classic; Medizintechnik Gulden), delivering 16 impulsive taps at intervals of 0.25 seconds. The accelerometer recorded responses at a 20 000 Hz sampling rate along 3-axes: x (mesiodistal), y (buccolingual), and z (implant

Figure 1. Jaw models with implant placement at site of first molar.

Figure 2. Custom-made surgical guide designed for precise and standardized implant placement in jaw models.

long axis) (Fig. 3). To reduce variation from tapping force and angle, frequency response functions (FRFs) were normalized to the maximum amplitude.

To simulate varying degrees of screw loosening, the abutment screw was initially tightened to 15 Ncm (0-degree loosening). It was then incrementally loosened in 5-degree steps up to 30 degrees, creating 6 loosening conditions: 5-degree, 10-degree, 15-degree, 20-degree, 25-degree, and 30-degree. For the intact condition, 20 vibration cycles (320 taps) were applied per specimen, while loosened conditions were tested with 4 vibration cycles each (384 taps total). FRFs were recorded for all 7 conditions, with resonance frequencies captured along all 3-axes.

Supervised learning models were developed using a random forest algorithm implemented via a machine learning library (Scikit-learn, version 0.24.1; Python Software Foundation) with 100 decision trees and default parameters (Fig. 4). Two classification tasks were conducted. For the binary classification, 320 intact specimens (0- degree) were labeled as 0, and 384 loosened specimens (64 for each of the 6 loosening angles from 5 degrees to 30 degrees) were combined and labeled as 1. For the multiclass classification, 64 specimens from each of the 7 conditions (0 degree to 30 degrees in 5-degree increments) were labeled from 0 to 6, resulting in 448 specimens in total. The datasets were split into 80% training and 20% testing sets. Model performance was assessed using accuracy metrics and confusion matrices, while feature importance analyses identified key

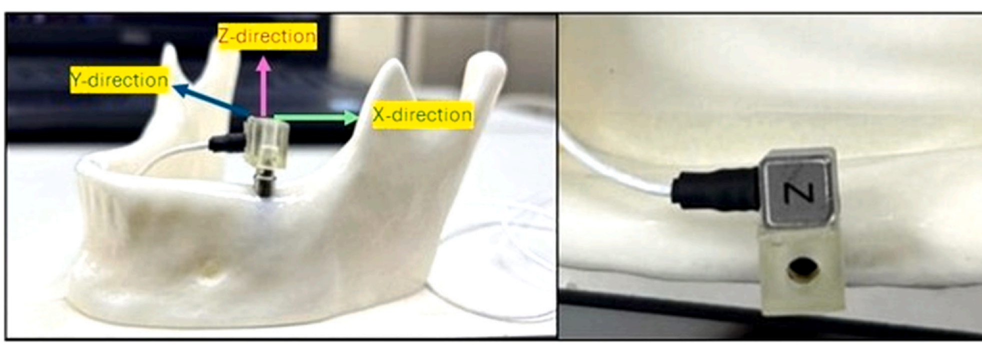

Figure 3. Three-dimensional accelerometer sensor installation on abutment and definition of direction on mandibular model.

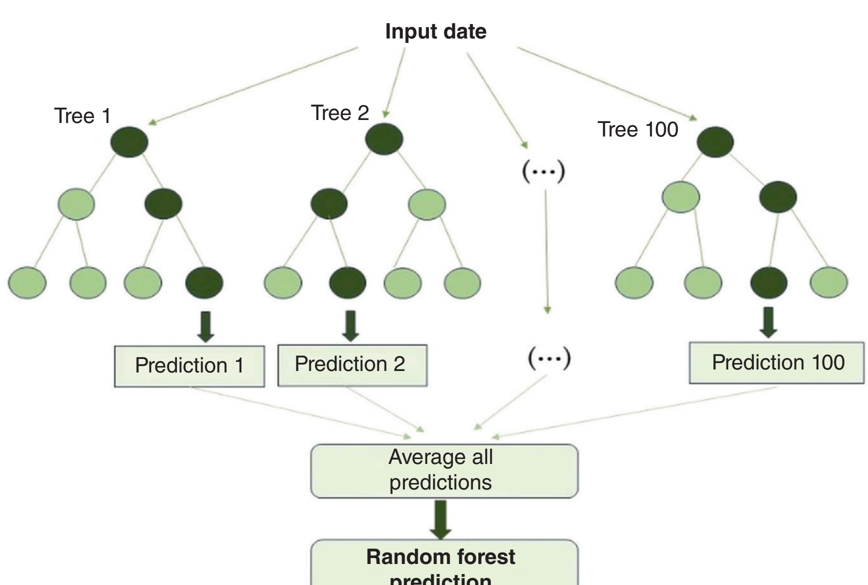

Figure 4. Random forest architecture.

Table 1. Architecture of convolutional autoencoder (CAE)

No.	Layer Type	Details of Parameters
1	Input layer	Node size=192 (1-dimensional vector)
2	Convolution layer	Filters=32, Kernel size=5
3	Convolution layer	Filters=32, Kernel size=5, Stride=1
4	Convolution layer	Filters=32, Kernel size=5, Strides=2
5	Convolution layer	Filters=64, Kernel size=5, Stride=1
6	Convolution layer	Filters=64, Kernel size=5, Strides=2
7	Convolution layer	Filters=128, Kernel size=5, Strides=2
8	Convolution layer	Filters=128, Kernel size=5, Strides=2
9	Convolution layer	Filters=128, Kernel size=5, Strides=2
10	Flatten layer	Node size=768 (6×128)
11	Dense layer	Node size=128
12	Dense layer	Node size=768
13	Reshape layer	Shape=6, 128
14	Convolution Transpose layer	Filters=128, Kernel size=5, Strides=2
15	Convolution Transpose layer	Filters=128, Kernel size=5, Strides=2
16	Convolution Transpose layer	Filters=128, Kernel size=5, Strides=2
17	Convolution Transpose layer	Filters=64, Kernel size=5, Strides=2
18	Convolution Transpose layer	Filters=64, Kernel size=5, Stride=1
19	Convolution Transpose layer	Filters=32, Kernel size=5, Strides=2
20	Convolution Transpose layer	Filters=32, Kernel size=5, Stride=1
21	Conv. Trans. layer (Output)	Filters=1, Kernel size=5, Activation=Sigmoid

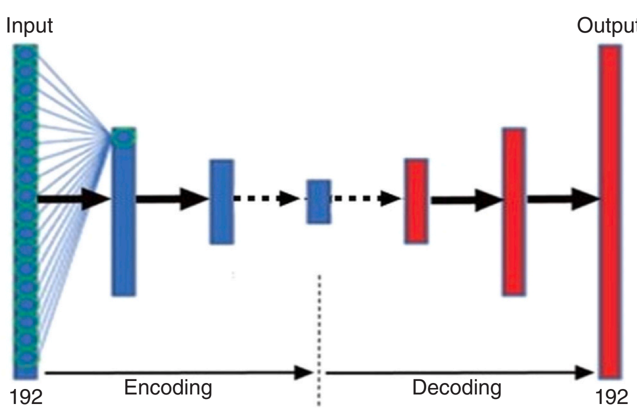

Figure 5. Schematic diagram of convolutional autoencoder.

resonance frequency features associated with screw loosening detection. To confirm reliability, Random Forest and Neural Network classifications were repeated across 200 trials.

For unsupervised learning, a convolutional autoencoder (CAE) was constructed as shown in Table 1 and Figure 5 using a deep learning framework (TensorFlow, version 2.8.0; Google LLC) with a neural network library (Keras, version 2.8.0; Google LLC). The CAE performed data compression and reconstruction with a 1-dimensional CNN, including a convolution layer to extract local features, a compression layer with strides of 2, a fully connected layer, and an up-sampling layer to increase resolution.[20] The rectified linear unit (ReLU) activation function was used throughout, except for the final layer, which used a sigmoid function. The model was trained to match input and output using mean squared error as the loss function, with 500 epochs, a learning rate of 0.001, Adam optimizer, and a batch size of 16. Frequency response functions from intact implants served as the baseline condition, while the dataset comprised 64 specimens for each of the 7 loosening angles. To address data variability, evaluations were repeated over 200 trials. Training stability was assessed by plotting loss functions using 80% of the data for training and 20% for validation, with epochs on the x-axis and loss values on the y-axis.

To enhance anomaly detection, a moving average filter with a window size of 5 consecutive frequency bins (corresponding to approximately 781 Hz) was applied to both input and output FRFs. Noise effects were mitigated by subtracting 0.1 from the values, with negative results set to zero, the anomaly score e was calculated as $e = \frac{\sum_{i=1}^{192} | f_i - g_i |}{\sum_{i=1}^{192} g_i}$, where fi and gi (1<i<192) are the input and reconstructed output frequency response functions, respectively. A threshold for abnormality was defined as the top 10% of anomaly scores from intact specimens, ensuring about 90% confidence in normal classification. Specimens exceeding this threshold were classified as abnormal, indicating potential screw loosening. Small variations in the threshold had minimal impact on results, showing that precise tuning was not critical for model performance.

RESULTS

The results demonstrated the effectiveness of the proposed methods in detecting and classifying different degrees of screw loosening across various implant–abutment connection designs. Visual interpretation of the frequency response function (FRF) alone provided limited diagnostic value, as spectral changes associated with loosening are subtle and difficult to interpret clinically. Therefore, machine learning was applied to extract discriminative features from FRF data for

Table 2. Confusion matrices for binary classification using random forest model: conical connection design. A, First specimen. B, Second specimen

A	Predicted value		
Real value		1	2
	1	64.3	0.0
	2	0.1	76.6
B	Predicted value		
Real value		1	2
	1	64.6	0.2
	2	0.2	76.0

Table 3. Confusion matrices for binary classification using neural network model: conical connection design. A, First specimen. B, Second specimen

A	Predicted value		
Real value		1	2
	1	64.3	0.0
	2	0.1	76.6
B	Predicted value		
Real value		1	2
	1	64.0	0.0
	2	0.1	76.9

classification. Representative FRFs for the 3 connection designs under intact and loosened conditions are shown in Supplemental Figures 1 to 3 (available online).

Supervised learning models using Random Forest and Neural Network algorithms classified screw loosening based on triaxial vibration patterns in the conical connection design. For binary classification, the Random Forest achieved accuracies of 100% and 99.7% for the first and second specimens (Table 2), respectively, while the Neural Network achieved 100% and 99.9% (Table 3). For multiclass classification, accuracies were 83.7% and 90.1% with Random Forest (Table 4), and 82.8% and 89.1% with the Neural Network (Table 5). Feature importance analysis indicated that resonance frequencies along all spatial axes were consistently critical for distinguishing loosening severity (Figs. 6, 7).

Unsupervised learning was conducted using a CAE trained on triaxial frequency responses and evaluated across 7 screw-loosening conditions. Anomaly scores, shown in Figure 8, indicate the degree of deviation from the intact state. A threshold based on the top 10% of intact-specimen scores identified abnormal conditions. Even the 5-degree loosening consistently exceeded this threshold, demonstrating the CAE's high sensitivity to subtle changes in implant–abutment stability.

Supervised learning analysis using Random Forest and Neural Network models was performed to evaluate screw loosening in 2 internal tri-channel specimens. In the binary classification, both models achieved high accuracy, with Random Forest reaching 100% and 99.9% (Table 6) and Neural Network reaching 100% and 99.7% (Table 7). Confusion matrices confirmed reliable separation between intact and loosened conditions. For multiclass classification, Random Forest achieved accuracies of 89.8% and 86.7% (Table 8), while Neural Network achieved 91.6% and 86.7% (Table 9). Feature importance analysis (Figs. 9, 10) consistently highlighted resonance frequencies across all axes as the most relevant features for detecting and classifying loosening severity.

Unsupervised learning analysis was performed using a CAE trained on x-, y-, and z-axis frequency responses. The CAE evaluated all screw loosening conditions, with results shown in Figure 11. A threshold set at the top 10% of anomaly scores from the intact condition served to identify abnormal states. In both specimens, the 5-degree loosening condition consistently exceeded this threshold, demonstrating the CAE's sensitivity to subtle deviations from the intact state.

Supervised learning analysis using Random Forest and Neural Network models was performed on 2 external hexagonal connection specimens. In the binary classification, Random Forest achieved accuracies of 99.4% and 98.3% (Table 10), while Neural Network

Table 4. Confusion matrices for multiclass classification using random forest model: conical connection design, A, First specimen. B, Second specimen

A	Predicted value							
Real value		0	1	2	3	4	5	6
	0	12.7	0.0	0.0	0.0	0.0	0.0	0.0
	1	0.2	11.7	1.0	0.0	0.2	0.0	0.0
	2	0.0	1.1	9.2	2.0	0.0	0.1	0.3
	3	0.0	0.1	1.3	11.3	0.0	0.0	0.1
	4	0.0	0.0	0.0	0.0	9.4	3.0	0.3
	5	0.0	0.0	0.0	0.0	3.4	9.3	0.2
	6	0.0	0.3	0.2	0.0	0.7	0.3	11.7
B	Predicted value							
Real value		0	1	2	3	4	5	6
	0	13.0	0.0	0.0	0.0	0.0	0.0	0.0
	1	0.0	12.8	0.0	0.0	0.0	0.0	0.0
	2	0.1	0.0	10.1	1.5	0.4	0.4	0.0
	3	0.1	0.0	1.1	10.5	1.0	0.3	0.0
	4	0.0	0.0	0.3	1.1	11.1	0.4	0.0
	5	0.0	0.0	1.2	0.5	0.2	11.0	0.0
	6	0.0	0.0	0.0	0.0	0.0	0.1	12.5

Table 5. Confusion matrices for multiclass classification using neural network model: conical connection design. A, First specimen. B, Second specimen

A	Predicted value							
Real value		0	1	2	3	4	5	6
	0	12.9	0.0	0.0	0.0	0.0	0.0	0.0
	1	0.0	10.7	1.3	0.1	0.1	0.1	0.2
	2	0.0	1.3	9.7	2.0	0.0	0.0	0.1
	3	0.0	0.2	1.8	10.9	0.0	0.0	0.1
	4	0.0	0.0	0.0	0.0	9.7	2.6	0.7
	5	0.0	0.0	0.0	0.0	2.4	9.7	0.5
	6	0.0	0.1	0.1	0.1	1.0	0.8	10.7
B	Predicted value							
Real value		0	1	2	3	4	5	6
	0	13.0	0.0	0.0	0.0	0.0	0.0	0.0
	1	0.0	12.8	0.0	0.0	0.0	0.0	0.0
	2	0.0	0.0	10.1	1.4	0.5	0.9	0.0
	3	0.0	0.0	0.6	10.4	0.9	0.6	0.0
	4	0.0	0.0	0.6	1.0	11.1	0.5	0.0
	5	0.0	0.0	1.4	0.9	0.2	10.1	0.0
	6	0.0	0.0	0.0	0.0	0.0	0.0	12.6

achieved 99.8% and 99.6% (Table 11). Confusion matrices confirmed reliable separation between intact and loosened conditions. For multiclass classification, Random Forest reached 94.5% and 89.9% (Table 12), whereas Neural Network achieved 95.3% and 85.4% (Table 13). Feature importance analysis (Figs. 12, 13) consistently demonstrated that resonance frequencies along the x, y, and z axes were the most critical features for detecting and grading screw loosening severity.

Unsupervised learning analysis was performed using a CAE trained on frequency responses along the x, y, and z axes. Anomaly scores for all screw loosening conditions are shown in Figure 14. A threshold set at the top 10% of scores from the intact condition identified

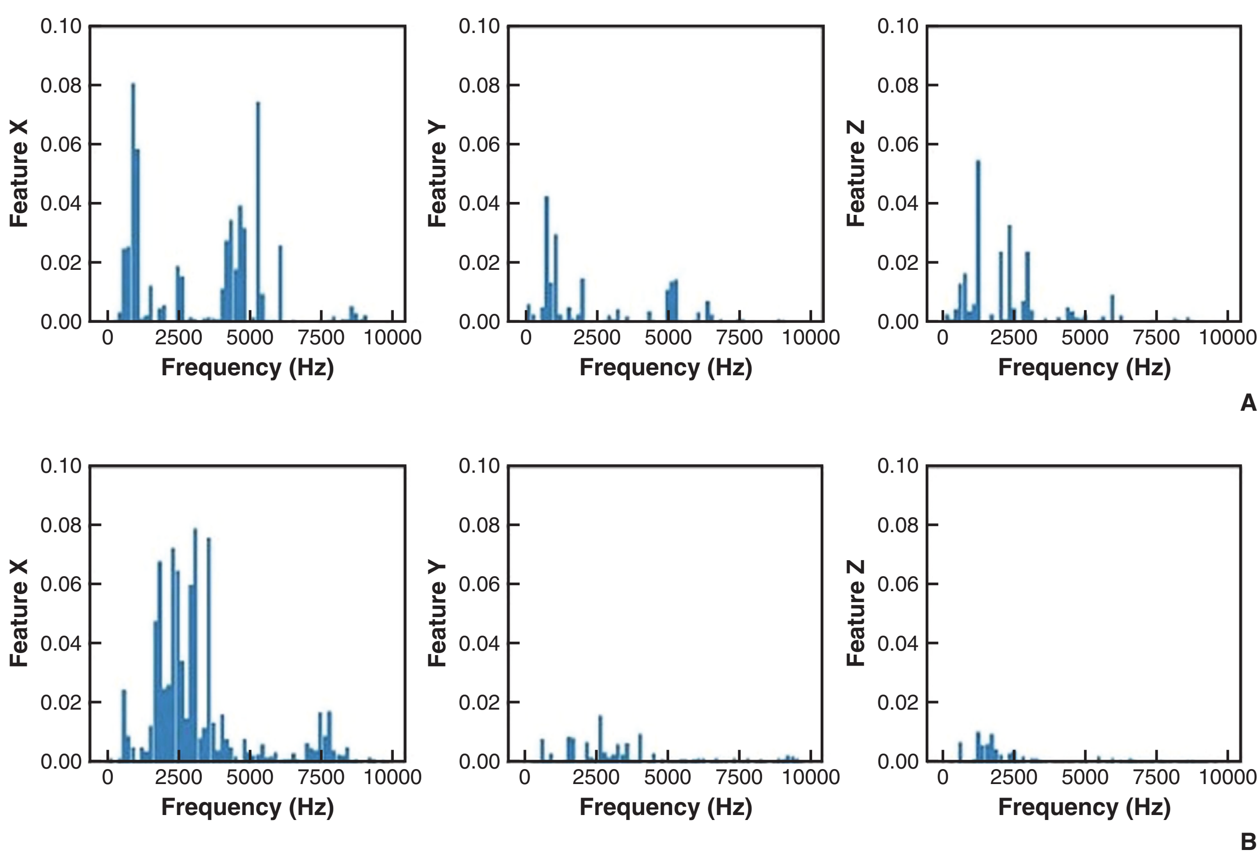

Figure 6. Feature importance analysis from random forest algorithm for detecting screw loosening in conical connection design after testing intact and abnormal classes. A, First specimen. B, Second specimen.

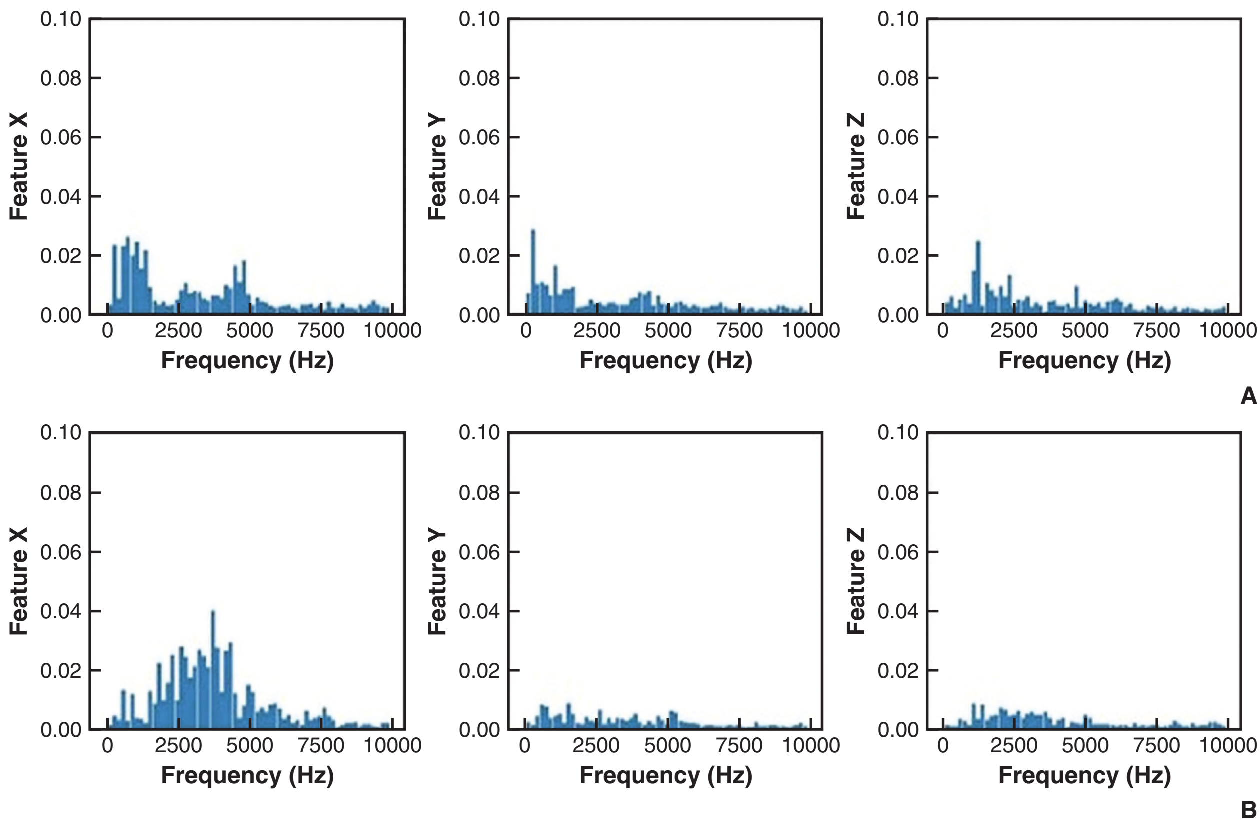

Figure 7. Feature importance analysis from random forest algorithm for detecting screw loosening in conical connection design after testing 7 screw loosening conditions. A, First specimen. B, Second specimen.

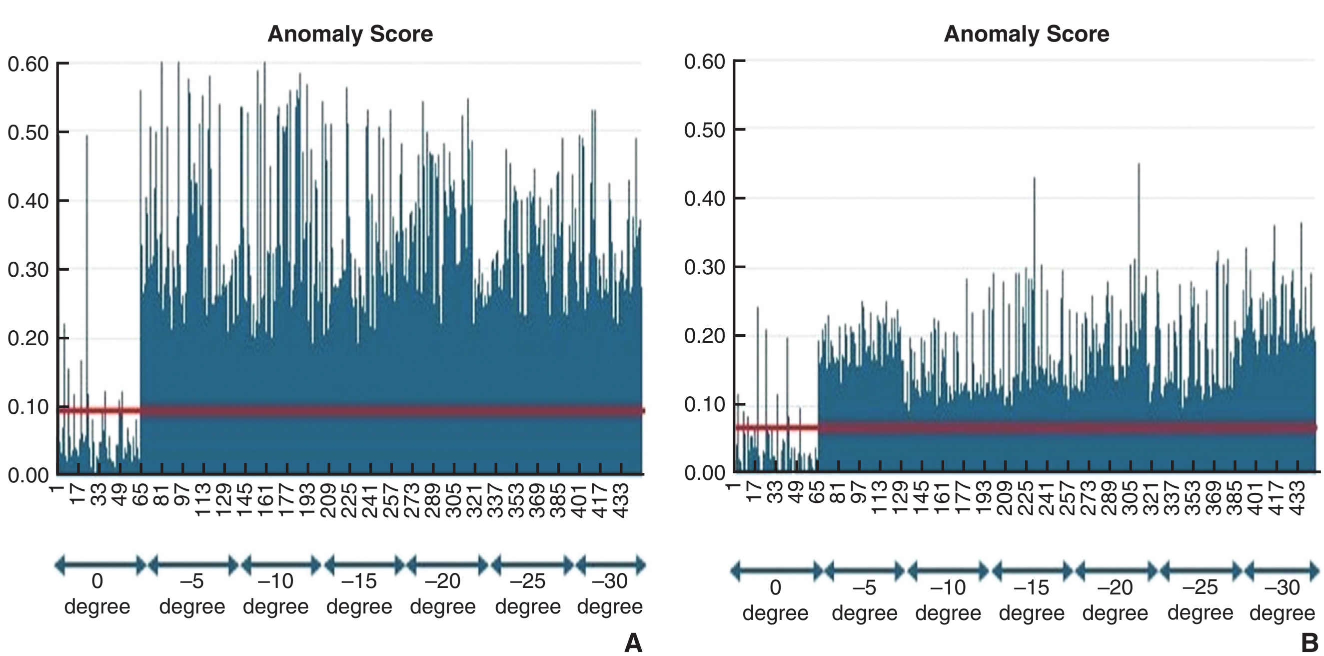

Figure 8. Frequency response anomaly score detection for various degrees of screw loosening in conical connection design. A, First specimen. B, Second specimen.

Table 6. Confusion matrices for binary classification using random forest model: internal tri channel connection design. A, First specimen. B, Second specimen

A	Predicted value		
Real value		1	2
	1	61.7	0.0
	2	0.0	77.2
B	Predicted value		
Real value		1	2
	1	64.7	0.1
	2	0.0	76.1

Table 7. Confusion matrices for binary classification using neural network model: internal tri channel connection design. A, First specimen. B, Second specimen

A	Predicted value		
Real value		1	2
	1	62.0	0.0
	2	0.0	77.0
B	Predicted value		
Real value		1	2
	1	63.9	0.2
	2	0.3	76.7

abnormal states, with the 5-degree loosening condition consistently exceeding this threshold.

Table 14 summarizes the CAE performance across 200 trials for each implant condition, with accuracy defined as the percentage of correctly detected loosened specimens (384 per trial). The CAE achieved near 100% accuracy for all implant types and loosening angles, with external hexagonal connections slightly lower at 92%, still clinically acceptable. The coefficient of variation was approximately 7%, indicating strong consistency and reproducibility. These results support the potential of this unsupervised approach for reliable screw loosening detection across implant designs. Training and validation loss functions were plotted to confirm model convergence and evaluate overfitting risk, showing stable convergence without divergence between curves, indicating appropriate generalization to unseen data (Supplemental Figs. 4–6, available online).

DISCUSSION

The null hypothesis that RFA combined with machine learning would not reliably detect screw loosening across different implant–abutment connections was rejected, as the method provided early, accurate and noninvasive screw loosening detection in conical, internal tri-channel, and external hexagonal designs. RFA results revealed distinct patterns for each connection type, which can be attributed to the inherent mechanical and structural characteristics of each implant system. Biomechanical studies[21,22] have shown that these connections exhibit different torque–displacement responses, supporting the observed variations in vibrational behavior.

The conical connection used a tapered design that created a friction fit between the implant and abutment, providing greater surface contact and a self-locking mechanism that enhanced stability when fully tightened.[23] Mechanical analyses using analytical and finite element methods[23,24] have shown that contact pressure and frictional engagement determine the pull-out force and loosening torque and that minor relative movements reduce friction, leading to decreased rigidity and increased vibrational mobility. Additionally, vertical discrepancies of 22.6 to 62.2 µm can occur when the abutment is not fully seated, reducing the engagement of antirotational and antibending features and compromising stability.[25] When loosening occurs, the taper permits small displacements between implant and abutment, diminishing frictional stability and increasing resonance amplitude,[12] reflecting decreased mechanical stiffness at the interface.

Table 8. Confusion matrices for multiclass classification using random forest model: internal tri-channel connection design. A, First specimen. B, Second specimen

A	Predicted value							
Real value		0	1	2	3	4	5	6
	0	12.9	0.0	0.0	0.0	0.0	0.0	0.0
	1	0.0	10.8	0.8	0.1	1.0	0.0	0.0
	2	0.0	1.0	10.3	1.3	0.2	0.0	0.0
	3	0.0	1.0	2.1	9.3	0.5	0.0	0.0
	4	0.0	0.3	0.3	0.5	11.9	0.0	0.0
	5	0.0	0.0	0.1	0.0	0.1	12.9	0.0
	6	0.0	0.0	0.0	0.0	0.0	0.0	12.8
B	Predicted value							
Real value		0	1	2	3	4	5	6
	0	12.2	0.1	0.0	0.0	0.0	0.0	0.1
	1	0.0	13.0	0.0	0.0	0.0	0.0	0.0
	2	0.0	0.0	12.3	0.2	0.0	0.0	0.0
	3	0.0	0.0	0.1	10.4	2.7	0.0	0.0
	4	0.0	0.0	0.1	2.8	10.2	0.0	0.0
	5	0.1	0.0	0.0	0.0	0.0	10.3	2.5
	6	0.0	0.0	0.0	0.0	0.0	3.0	9.7

Table 9. Confusion matrices for multiclass classification using neural network model: internal tri-channel connection design. A, First specimen. B, Second specimen

A	Predicted value							
Real value		0	1	2	3	4	5	6
	0	12.8	0.0	0.0	0.0	0.0	0.0	0.0
	1	0.0	11.2	1.0	0.3	0.5	0.0	0.0
	2	0.0	1.2	10.2	1.1	0.1	0.0	0.0
	3	0.0	0.4	1.3	10.7	0.7	0.0	0.0
	4	0.0	0.2	0.0	0.5	12.3	0.0	0.0
	5	0.0	0.0	0.1	0.0	0.0	12.4	0.0
	6	0.0	0.1	0.0	0.0	0.0	0.1	12.6
B	Predicted value							
Real value		0	1	2	3	4	5	6
	0	12.2	0.1	0.0	0.0	0.0	0.0	0.1
	1	0.0	13.0	0.0	0.0	0.0	0.0	0.0
	2	0.0	0.0	12.3	0.2	0.0	0.0	0.0
	3	0.0	0.0	0.1	10.4	2.7	0.0	0.0
	4	0.0	0.0	0.1	2.8	10.2	0.0	0.0
	5	0.1	0.0	0.0	0.0	0.0	10.3	2.5
	6	0.0	0.0	0.0	0.0	0.0	3.0	9.7

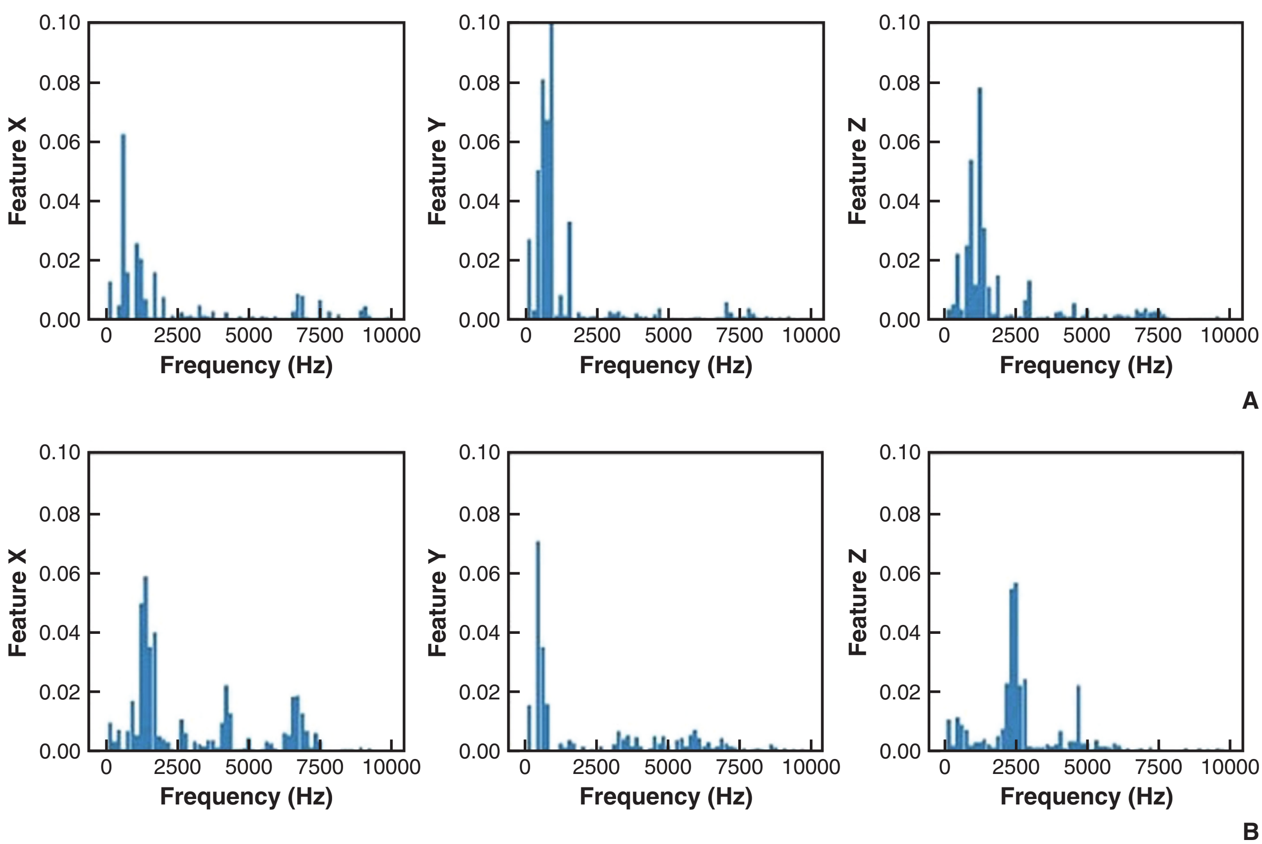

Figure 9. Feature importance analysis from random forest algorithm for detecting screw loosening in internal tri-channel connection design after testing intact and abnormal classes. A, First specimen. B, Second specimen.

Internal tri-channel and external hexagonal connections rely on mechanical locking features such as screws or interlocking channels rather than friction, resulting in less surface contact than conical connections. Stability depends on the engagement of these locking elements, which weakens when loosening occurs. Previous studies[26,27] have reported that internal connections exhibit greater microdisplacement than external hexagonal connections once preload is lost because of their geometry and wider contact area. This microdisplacement allows the internal connection to deform more under functional loading, amplifying vibrational responses detectable by Periotest or resonance frequency analysis. In contrast, the external

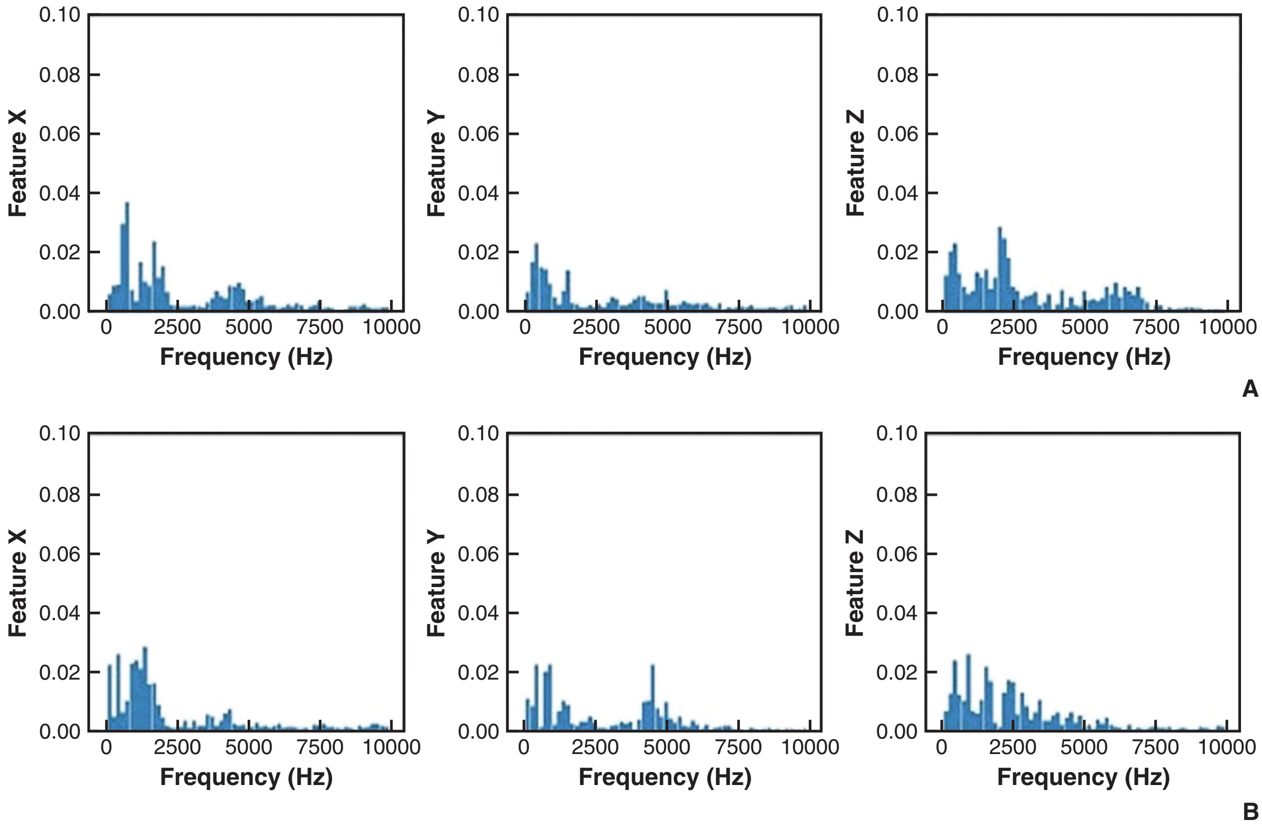

Figure 10. Feature importance analysis from random forest algorithm for detecting screw loosening in internal tri-channel connection design after testing 7 screw loosening conditions. A, First specimen. B, Second specimen.

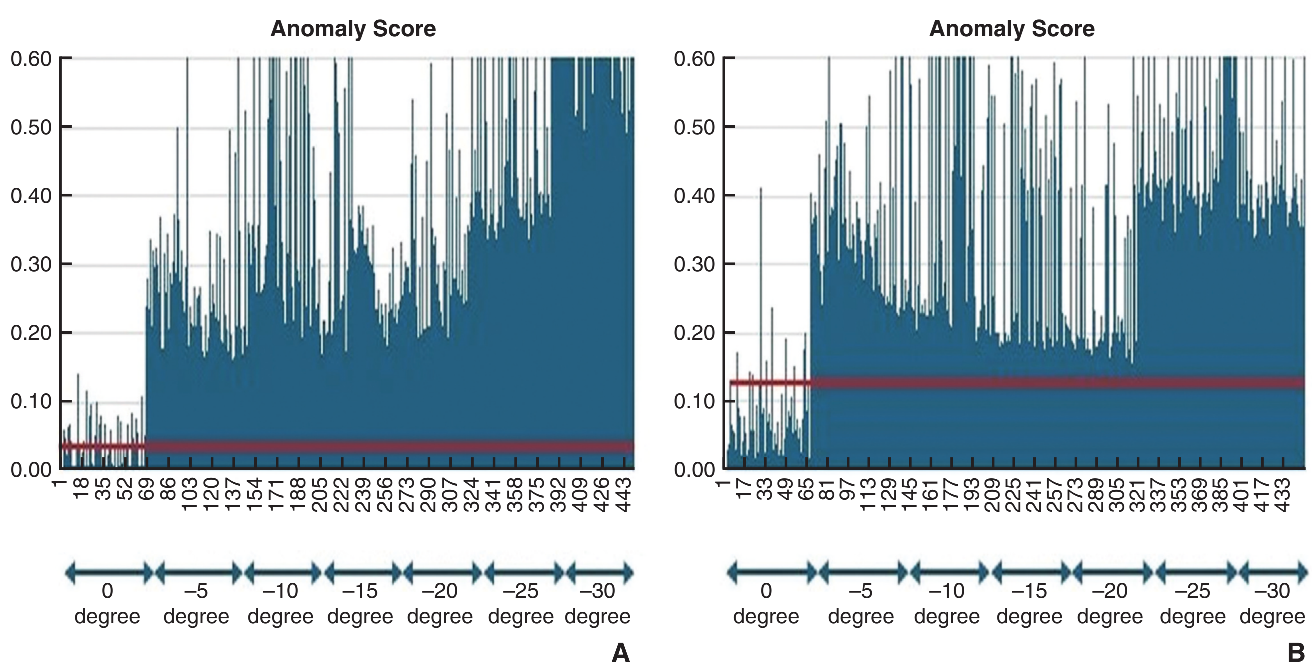

Figure 11. Frequency response anomaly score detection for various degrees of screw loosening in internal tri channel connection design. A, First specimen. B, Second specimen.

Table 10. Confusion matrices for binary classification using random forest model: external hexagonal design. A, First specimen. B, Second specimen

A	Predicted value		
Real value		1	2
	1	63.3	0.8
	2	0.1	76.8
B	Predicted value		
Real value		1	2
	1	62.7	0.9
	2	1.4	76.0

Table 11. Confusion matrices for binary classification using neural network model: external hexagonal design. A, First specimen. B, Second specimen

A	Predicted value		
Real value		1	2
	1	63.6	0.2
	2	0.0	77.2
B	Predicted value		
Real value		1	2
	1	64.0	0.1
	2	0.4	76.5

hexagonal design, with a smaller contact area and screw-based stabilization, exhibits less displacement and less pronounced vibrational changes after loosening.[28] These differences highlight how implant–abutment connection geometry influences both mechanical stability and vibrational behavior under screw loosening.

High accuracy in detecting and classifying screw loosening can be attributed to several factors. Each implant–abutment connection design exhibits a unique resonance frequency pattern under different loosening conditions, providing discriminative input for machine learning. Triaxial accelerometer data capture subtle vibrations across all 3 axes, offering a rich multidimensional feature set.[29] Random Forest, which estimates feature importance by averaging impurity reduction across trees, identifies key features and enhances model performance.[17] In this study, the algorithm achieved perfect accuracy for binary classification and 83% to 92% for multiclass classification. Feature importance consistently highlighted resonance frequencies along the x, y, and z axes, supporting their utility in detecting varying degrees of loosening.

The CAE provided valuable insight by detecting anomalies associated with screw loosening,[18] Well-established for unsupervised anomaly detection, it identified deviations from the intact state even at minor loosening (5 degrees), demonstrating its potential to complement supervised techniques without labeled data. Trained on x-, y-, and z-axis frequency responses, the CAE consistently detected subtle vibrational changes across all implant–abutment connection designs. A threshold set at the top 10% of anomaly scores from intact specimens effectively distinguished normal from abnormal conditions while minimizing false positives.

Limitations of this study included the in vitro design that did not fully replicate clinical conditions, where factors such as bone density, soft tissue, saliva, occlusal loading, and patient movement may influence resonance frequency responses. Only 6 implants (2 per connection type) were tested, limiting generalizability and statistical power; however, multiple measurements per implant and repeated machine learning analyses strengthened the dataset. Loosening was simulated using incremental rotation (0 degree to 30 degrees), which did not capture gradual fatigue, occlusal forces, or microleakage contributing to clinical screw loosening. Torque loss was not measured alongside angular loosening; incorporating such measurements would provide direct mechanical

Table 12. Confusion matrices for multiclass classification using random forest model: external hexagonal connection design. A, First specimen. B, Second specimen

A	Predicted value							
Real value		0	1	2	3	4	5	6
	0	12.5	0.2	0.0	0.1	0.0	0.0	0.0
	1	0.0	12.6	0.2	0.0	0.0	0.0	0.0
	2	0.1	0.0	11.3	1.1	0.0	0.0	0.0
	3	0.0	0.0	0.7	12.0	0.0	0.0	0.0
	4	0.0	0.0	0.0	0.0	12.4	0.1	0.7
	5	0.0	0.0	0.0	0.0	0.0	12.0	0.7
	6	0.0	0.0	0.0	0.0	0.5	0.4	12.3
B	Predicted value							
Real value		0	1	2	3	4	5	6
	0	12.2	0.3	0.1	0.0	0.0	0.0	0.0
	1	0.3	8.1	3.7	0.4	0.0	0.0	0.0
	2	0.2	3.6	9.3	0.0	0.0	0.0	0.0
	3	0.1	0.1	0.1	12.9	0.0	0.0	0.0
	4	0.0	0.0	0.0	0.0	12.9	0.0	0.0
	5	0.0	0.0	0.0	0.0	0.0	12.7	0.0
	6	0.0	0.0	0.0	0.0	0.0	0.2	12.8

Table 13. Confusion matrices for multiclass classification using random forest model: external hexagonal connection design. A, First specimen. B, Second specimen

A	Predicted value							
Real value		0	1	2	3	4	5	6
	0	12.1	0.3	0.1	0.0	0.0	0.0	0.0
	1	0.1	12.7	0.2	0.0	0.0	0.0	0.0
	2	0.2	0.1	11.5	0.9	0.0	0.0	0.0
	3	0.0	0.0	0.8	12.6	0.0	0.0	0.0
	4	0.0	0.0	0.0	0.0	12.4	0.0	0.1
	5	0.0	0.0	0.0	0.0	0.2	12.4	0.6
	6	0.0	0.0	0.0	0.0	0.3	0.4	12.2
B	Predicted value							
Real value		0	1	2	3	4	5	6
	0	12.4	0.2	0.4	0.0	0.0	0.0	0.0
	1	0.5	6.5	5.6	0.5	0.0	0.0	0.0
	2	0.7	4.5	7.2	0.2	0.0	0.0	0.0
	3	0.0	0.2	0.1	12.5	0.0	0.0	0.0
	4	0.0	0.0	0.0	0.0	12.8	0.0	0.0
	5	0.0	0.0	0.0	0.0	0.0	12.8	0.0
	6	0.0	0.0	0.0	0.0	0.1	0.1	12.8

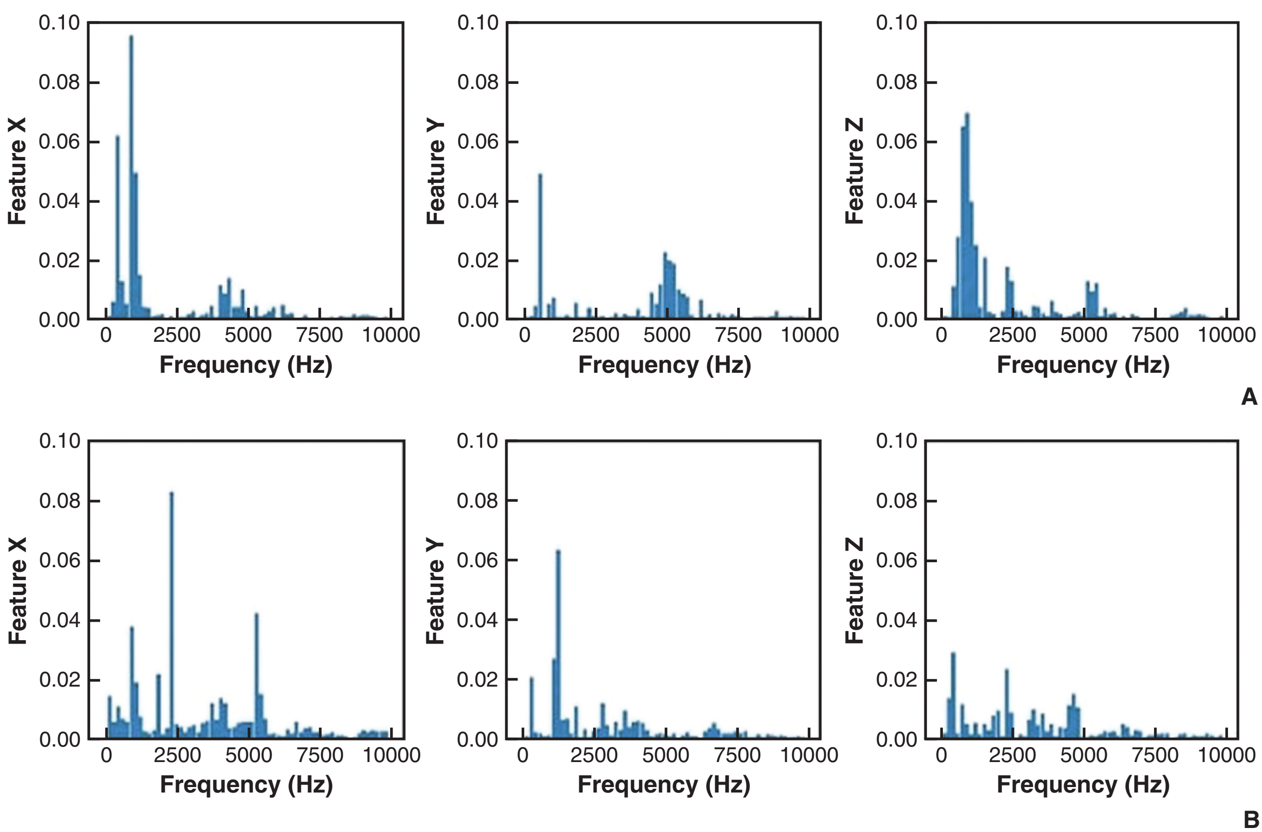

Figure 12. Feature importance analysis from random forest algorithm for detecting screw loosening in external hexagonal connection design after testing intact and abnormal classes. A, First specimen. B, Second specimen.

validation. External validation using independent datasets is also needed to ensure model generalizability. Despite these constraints, the findings provided proof-of-concept evidence that RFA combined with machine learning can detect screw loosening. Future studies should include larger sample sizes, additional connection types, multi-unit restorations, cyclic fatigue testing, and in vivo conditions to validate reproducibility and clinical applicability. Integration with other noninvasive diagnostic tools and longitudinal monitoring may further improve early detection and long-term implant outcomes.

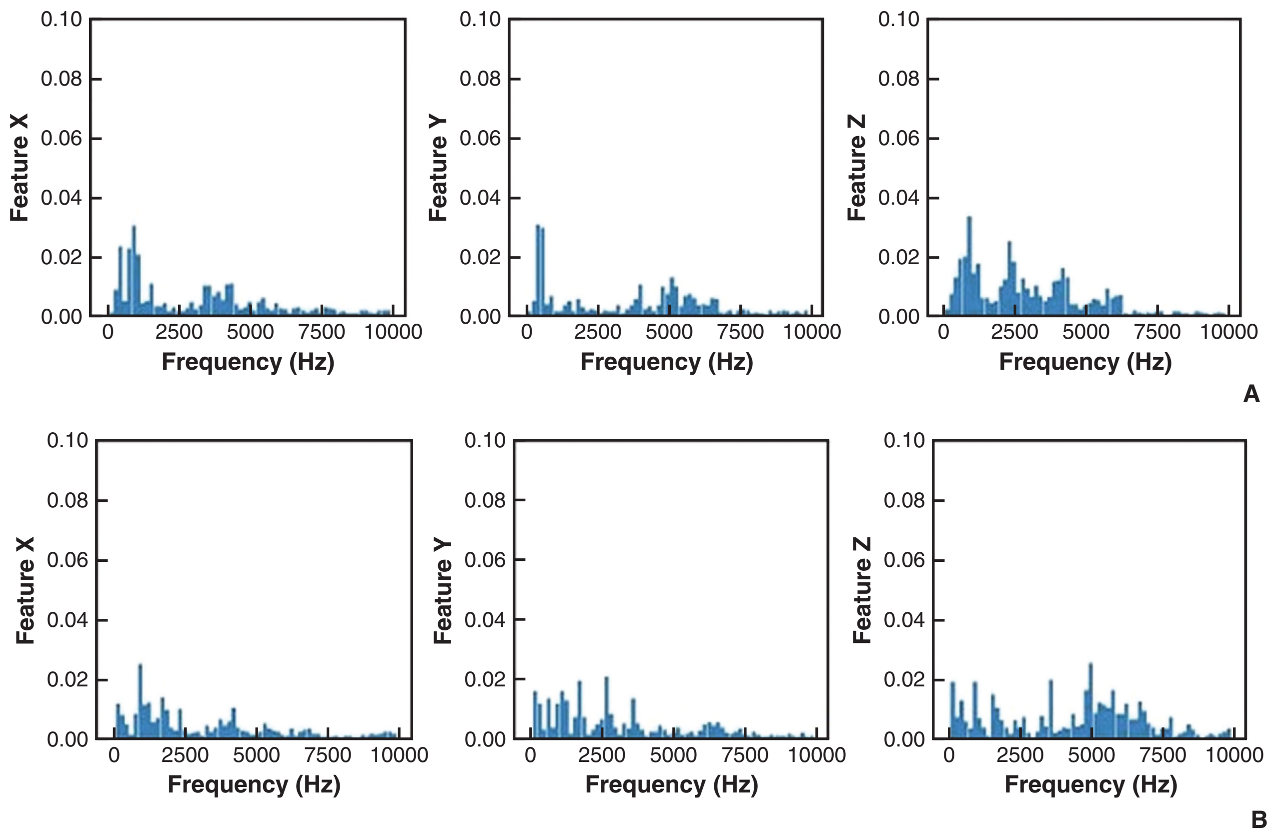

Figure 13. Feature importance analysis from random forest algorithm for detecting screw loosening in external hexagonal connection design after testing 7 screw loosening conditions. A, First specimen. B, Second specimen.

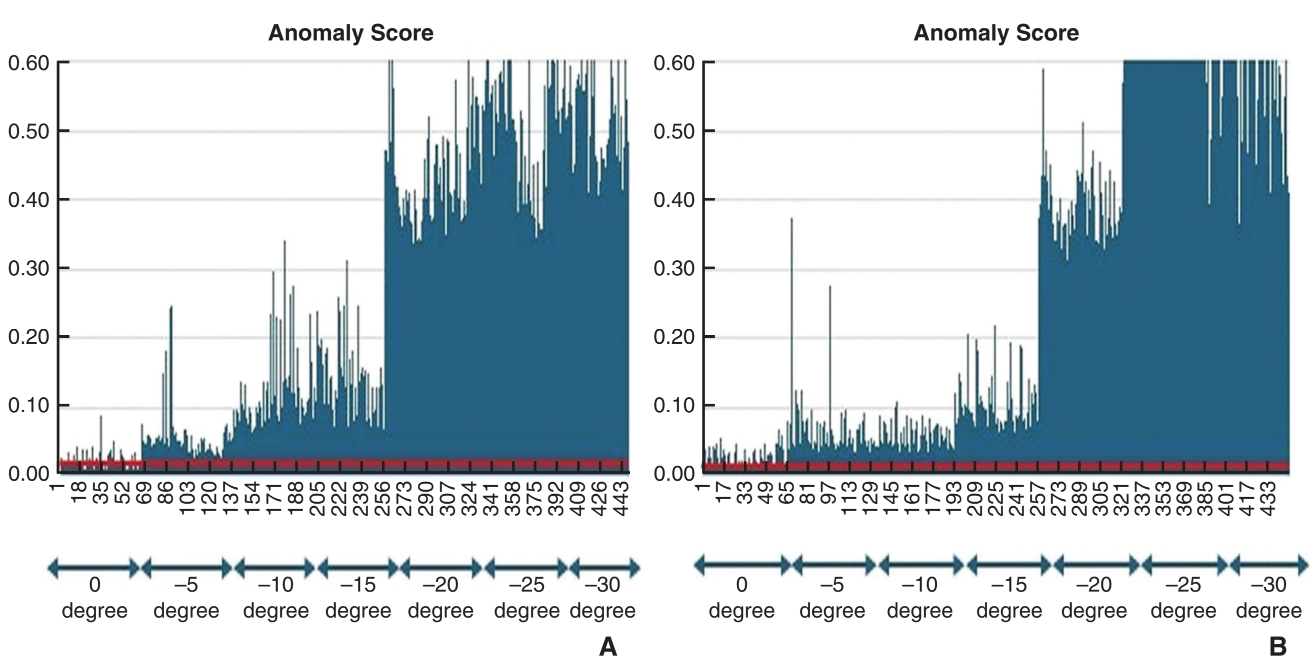

Figure 14. Frequency response anomaly score detection for various degrees of screw loosening in external hexagonal connection design. A, First specimen. B, Second specimen.

Table 14. Prediction accuracy for loosened conditions using convolutional autoencoder

	Conical (1st_specimen)	Conical (2nd_ specimen)	Internal Tri-Channel (1st_ specimen)	Internal Tri-Channel (2nd_ specimen)	External Hexagon (1st_ specimen)	External Hexagon (2nd_ specimen)
Mean from 200 trials	99.9%	98.4%	100.0%	99.3%	96.0%	92.2%
Coefficient of variation	0.5%	7.6%	0.1%	2.9%	4.3%	7.6%

CONCLUSIONS

Based on the findings of this in vitro study, the following conclusions were drawn:

1. Resonance frequency analysis (RFA) combined with machine learning effectively detected screw loosening across 3 implant–abutment connection designs: conical, internal tri-channel, and external hexagonal.
2. Distinct vibrational changes were observed with increasing loosening severity, and the machine learning models demonstrated high classification accuracy.
3. These results highlighted the potential of RFA with advanced data analysis as a noninvasive tool for early detection of screw instability; however, further studies under clinical conditions are needed to validate its applicability in patient care.

APPENDIX A. SUPPORTING INFORMATION

Supplemental data associated with this article can be found in the online version at doi:10.1016/j.prosdent.2025.12.007.

REFERENCES

1. Cavazos E, Bell FA. Preventing loosening of implant abutment screws. *J Prosthet Dent*. 1996;75:485–491.
2. Lee KY, Shin KS, Jung JH, Cho HW, Kwon KH, Kim YL. Clinical study on screw loosening in dental implant prostheses: A 6-year retrospective study. *J Korean Assoc Oral Maxillofac Surg*. 2020;46:116–124.
3. Kourtis S, Damanaki M, Kaitatzidou S, Kaitatzidou A, Roussou V. Loosening of the fixing screw in single implant crowns: Predisposing factors, prevention and treatment options. *J Esthet Restor Dent*. 2017;29:283–292.
4. Alsubaiy E. Abutment screw loosening in implants: A literature review. *J Family Med Prim Care*. 2020;9:5620–5625.
5. Sennerby L. Resonance frequency analysis for implant stability measurements: A review. *Integ Diagn Update*. 2015;1:1–8.
6. Hum S. Managing patients with a loose implant abutment screw. *J Can Dent Assoc*. 2014;80:e13.
7. Kim GY, Kim S, Chang JS, Pyo SW. Advancements in methods of classification and measurement used to assess tooth mobility: A narrative review. *J Clin Med*. 2024;13:1789.
8. Spirig JM, Sutter R, Götschi T, Farshad-Amacker NA, Farshad M. Value of standard radiographs, computed tomography, and magnetic resonance imaging of the lumbar spine in detection of intraoperatively confirmed pedicle screw loosening: A prospective clinical trial. *Spine J*. 2019;19:417–425.
9. Wu JC, Huang WC, Tsai HW, et al. Pedicle screw loosening in dynamic stabilization: Incidence, risk, and outcome in 126 patients. *Neurosurg Focus*. 2011;31:E10.
10. Meredith N, Alleyne D, Cawley P. Quantitative determination of the stability of the implant-tissue interface using resonance frequency analysis. *Clin Oral Implants Res*. 1996;7:261–267.
11. Xiao Y, Lv L, Xu Z, et al. Correlation between peri-implant bone mineral density and primary implant stability based on artificial intelligence classification. *Sci Rep*. 2024;14:4552.
12. Miyashita M, Ogawa T, Naito H, et al. Evaluation of implant screw loosening by resonance frequency analysis with triaxial piezoelectric pick-up: in vitro model and in vivo animal study. *Clin Oral Investig*. 2018;22:2129–2134.
13. Mikami K, Nemoto M, Nagura T, Nakamura M, Matsumoto M, Nakashima D. Machine learning-based diagnosis in laser resonance frequency analysis for implant stability of orthopedic pedicle screws. *Sensors (Basel)*. 2021;21:8352.
14. Nakashima D, Mikami K, Kikuchi S, et al. Laser resonance frequency analysis of pedicle screw stability: A cadaveric model bone study. *J Orthop Res*. 2021;39:2354–2363.
15. Gupta RK, Padmanabhan TV. Resonance frequency analysis. *Indian J Dent Res*. 2011;22:567–573.
16. Schwendicke F, Samek W, Krois J. Artificial intelligence in dentistry: Chances and challenges. *J Dent Res*. 2020;99:769–774.
17. Scornet E. Trees, forests, and impurity-based variable importance in regression. *Ann Inst Henri Poincaré Probab Stat*. 2023;59:257–289.
18. Suryawati E, Pardede HF, Zilvan V, et al. Unsupervised feature learning-based encoder and adversarial networks. *J Big Data*. 2021;8:45.
19. Qi J, Miyashita M, Ogawa T, Naito H, Sasaki K. Resonance frequency analysis for evaluation of the connecting condition between fixed prostheses and their abutment teeth: An in vitro and finite element analysis study. *J Prosthet Dent*. 2024;131:567–578.
20. Sammour SR, Naito H, Kimoto T, Sasaki K, Ogawa T. Anomaly detection of retention loss in fixed partial dentures using resonance frequency analysis and machine learning: An in vitro study. *J Prosthodont Res*. 2024;68:123–134.
21. Pessoa RS, Bezerra FJB, Sousa RM, Vander Sloten J, Casati MZ, Jaecques SVN. Biomechanical evaluation of platform switching: Different mismatch sizes, connection types, and implant protocols. *J Periodontol*. 2014;85:1222–1230.
22. Macedo JP, Pereira J, Vahey BR, et al. Morse taper dental implants and platform switching: The new paradigm in oral implantology. *Eur J Dent*. 2016;10:72–78.
23. Schmitt CM, Nogueira-Filho G, Tenenbaum HC, et al. Performance of conical abutment (Morse taper) connection implants: A systematic review. *J Biomed Mater Res A*. 2014;102:552–564.
24. Bozkaya D, Müftü S. Mechanics of the tapered interference fit in dental implants. *J Biomech*. 2003;36:1649–1658.
25. Kofron MD, Carstens M, Fu C, Wen HB. In vitro assessment of connection strength and stability of internal implant-abutment connections. *Clin Biomech*. 2019;65:58–65.
26. Atsumi M, Park SH, Wang HL. Methods used to assess implant stability: Current status. *Int J Oral Maxillofac Implants*. 2007;22:779–788.
27. Guda T, Ross TA, Lang LA, Millwater HR. Probabilistic analysis of preload in the abutment screw of a dental implant complex. *J Prosthet Dent*. 2008;100:193–202.
28. Feitosa PCP, de Lima APB, Silva-Concílio LR, Brandt WC, Claro Neves AC. Stability of external and internal implant connections after a fatigue test. *Eur J Dent*. 2013;7:155–161.
29. Zanetti EM, Ciaramella S, Calì M, et al. Modal analysis for implant stability assessment: sensitivity of this methodology for different implant designs. *Dent Mater*. 2018;34:1123–1133.

Corresponding author:
Prof Toru Ogawa
Division of Comprehensive Dentistry
Tohoku University Graduate School of Dentistry
4–1 Seiryo-machi
Aoba-ku, Sendai, Miyagi 980–8575
JAPAN
Email: toru.ogawa.d7@tohoku.ac.jp

https://doi.org/10.1016/j.prosdent.2025.12.007